RESEARCH ARTICLE

Biochar as electron donor for reduction of N_2O by *Paracoccus denitrificans*

Mª Blanca Pascual[1,2,*], Miguel Ángel Sánchez-Monedero[1], María L. Cayuela[1,†], Shun Li[3], Stefan B. Haderlein[3], Reiner Ruser[4] and Andreas Kappler[2]

[1]Department of Soil and Water Conservation and Waste Management, Centro de Edafología y Biología Aplicada del Segura (CEBAS-CSIC), Campus Universitario de Espinardo 30100 Murcia, Spain, [2]Geomicrobiology, Center for Applied Geosciences, University of Tübingen, Sigwartstrasse 10, 72074 Tübingen, Germany, [3]Environmental Mineralogy and Chemistry, Center for Applied Geosciences, University of Tübingen, Sigwartstrasse 10, 72074 Tübingen, Germany and [4]Institute of Crop Science, Department of Fertilization and Soil Matter Dynamics, University of Hohenheim, Fruwirthstraβe 20, 70599 Stuttgart, Germany

*Corresponding author: Department of Soil and Water Conservation and Waste Management, Centro de Edafología y Biología Aplicada del Segura (CEBAS-CSIC), Campus Universitario de Espinardo 30100 Murcia, Spain. Tel: +34 968396200; Fax: +34 968396213; E-mail: mb.pascualv@gmail.com, blanca.pascual@csic.es

One sentence summary: Nitrous oxide reduction by *Paracoccus denitrificans* has been found to be enhanced by biochar by means of its electron donating capacity.

ABSTRACT

Biochar (BC) has been shown to influence microbial denitrification and mitigate soil N_2O emissions. However, it is unclear if BC is able to directly stimulate the microbial reduction of N_2O to N_2. We hypothesized that the ability of BC to lower N_2O emissions could be related not only to its ability to store electrons, but to donate them to bacteria that enzymatically reduce N_2O. Therefore, we carried out anoxic incubations with *Paracoccus denitrificans*, known amounts of N_2O, and nine contrasting BCs, in the absence of any other electron donor or acceptor. We found a strong and direct correlation between the extent and rates of N_2O reduction with BC's EDC/EEC (electron donating capacity/electron exchange capacity). Apart from the redox capacity, other BC properties were found to regulate the BC's ability to increase N_2O reduction by *P. denitrificans*. For this specific BC series, we found that a high H/C and ash content, low surface area and poor lignin feedstocks favored N_2O reduction. This provides valuable information for producing tailored BCs with the potential to assist and promote the reduction of N_2O in the pursuit of reducing this greenhouse gas emissions.

Keywords: denitrification; charcoal; electron shuttle; redox; nitrous oxide; electron donating capacity

INTRODUCTION

Nitrous oxide (N_2O) is one of the main contributors to global warming among the greenhouse gases released by agricultural activities (IPCC 2014). Soils are the primary source of atmospheric N_2O and their contribution has been constantly increasing since pre-industrial times (Butterbach-Bahl *et al.* 2013). Recently, biochar (BC) soil amendments were proposed as an effective approach to tackle N_2O emissions in agro-ecosystems (Clough *et al.* 2013; Kammann *et al.* 2017). Biochar is created through the pyrolysis of biomass under high-temperature and low-oxygen conditions (Lehmann 2007). When added to soil, BC affects its microbial activity, physical structure and chemical properties, and is more recalcitrant to microbial decomposition than the original feedstock (Zhang *et al.* 2010; Keith, Singh and Singh 2011). Several meta-analyses have demonstrated that BC mitigates nitrogen (N) losses and reduces nitrous oxide (N_2O) emissions from soils (Cayuela *et al.* 2014; Borchard *et al.* 2019; Liu *et al.* 2019). Specifically, it changes the microbial community of nitrous oxide reducers (Harter *et al.* 2017; Krause *et al.* 2018). However, despite this research, the exact mechanisms of action are not fully understood (Weldon *et al.* 2019).

Paracoccus denitrificans is a model soil microorganism that is widely employed for bioenergetic studies. It is capable of denitrification down to its last step and rapidly reduces N_2O to N_2 with nitrate or nitrite as the electron acceptor and succinate, NADH, glucose, acetate or methanol as the electron donor (Stouthamer 1980; Kučera *et al.* 1983; Baumann *et al.* 1996; Felgate *et al.* 2012; Hahnke *et al.* 2014; Olaya-Abril *et al.* 2018). This denitrification reaction is catalyzed by the multicopper enzyme nitrous oxide reductase (N_2OR). This enzyme is encoded by a *nor/nos* gene cluster that drives the synthesis of the essential proteins required for its activity. The periplasmic *nosZ* protein is not always present in every denitrifying bacterium, which causes the blocking of N_2 production and the subsequent release of N_2O (Torres *et al.* 2016; Carreira, Pauleta and Moura 2017).

Several recent studies have demonstrated that BC stimulates the last step of denitrification, where N_2O is reduced to N_2. The suggested mechanisms have included the 'electron shuttle' theory (Cayuela *et al.* 2013; Fungo *et al.* 2019), the effect BC has over soil pH and N_2O residence time (Weldon *et al.* 2019), the involvement of BC redox active components (Chen *et al.* 2018) or its N_2O adsorption potential (Quin *et al.* 2015). Nevertheless, this last step is highly variable across BC types (Weldon *et al.* 2019; Yuan *et al.* 2019). When applied to soils, BC can affect N_2O dynamics through abiotic and/or biotic mechanisms. Biochar has been found to adsorb and abiotically reduce N_2O injected in sterilized soil columns (Quin *et al.* 2015), but also stores N_2O and stimulates microbial N_2O reduction (Harter *et al.* 2016). In addition, BC has been suggested to mediate redox reactions during biological denitrification, acting as a reducing agent (i.e. an electron donor) for denitrifying bacteria or as an electron shuttle. When functioning as an electron donor, reduced functional groups in BC are biologically oxidized and the electrons are donated to N-species that function as electron acceptors (Chen *et al.* 2018). When acting as an electron shuttle, BC is reversibly reduced and oxidized by both accepting and donating electrons. BC reduction proceeds by abiotic reductants or by reducing bacteria. Meanwhile, BC oxidation occurs either by abiotic electron acceptors or microorganisms that use these electrons for energy generation and/or CO_2 fixation (Xu *et al.* 2016; Yu *et al.* 2016). Both electron donor or electron shuttle functions are based on the presence of redox-active functional groups (quinones/hydroquinones) and redox-active aromatic structures that allow the presence of delocalized π-electrons in BC (Chen *et al.* 2014; Sun *et al.* 2017; Yuan *et al.* 2017), a property that differentiate them from other redox-active carbon rich materials such as humic substances (Wu *et al.* 2017). Nevertheless, the role of BC redox reactions for influencing N_2O emissions has not been experimentally verified with pure cultures of denitrifying bacteria or soil matrices yet (Yuan *et al.* 2019). The main difficulty in determining the role of BC during denitrification processes lies in its complex properties. These properties hinder the distinction between redox and other BC properties that could also be involved (e.g. its sorption capacity). The origin of BC's intricate properties is mainly controlled by the ratios of lignin, cellulose and hemicellulose in the feedstock as well as its pyrolysis production parameters (Zhao *et al.* 2013; Prévoteau *et al.* 2016). Based on previous studies, a link between BC characteristics and its ability to donate, accept, or in general, to transfer electrons can be envisaged. For instance, the presence of redox-active functional groups at the BC surface is the primary cause for the electron donation ability at low temperature possessed by BCs (Kappler *et al.* 2014; Yu *et al.* 2016; Sun *et al.* 2018). However, the conductivity of electrons through polycondensed aromatic structures dominates the transfer of electrons in BCs pyrolyzed at the highest treatment temperature (HTT) > 650°C, as these have a high degree of aromaticity (molar hydrogen/carbon, H/C, ratios < 0.3; Chen *et al.* 2014; Sun *et al.* 2017; Sun *et al.* 2018).

Previous studies have been carried out with a limited number of BCs, which do not allow their conclusions to be generalized. Consequently, the effect of BCs with contrasting redox properties on the microbe-catalyzed reduction of N_2O to N_2 remains unknown. It is therefore necessary to study the effect of different BC characteristics on microbial N_2O reduction. This would allow producing BC on demand by adjusting the feedstock utilized and the pyrolysis conditions to enhance their redox potential and boost N_2O-reducing bacteria activity.

Consequently, the main objective of our work was to evaluate the ability of dissimilar BCs to support N_2O reduction by *P. denitrificans* by means of their redox properties in the absence of any other C or electron source. Moreover, the effect of BCs modified by both ageing in soil and post-pyrolysis chemical treatment was evaluated. Our two hypotheses were (i) the use of BCs will lead to the reduction of N_2O to N_2 by *P. denitrificans* with an extent that depends on BC redox properties (i.e. their electron exchange capacity, EEC and electron donating capacity, EDC); (ii) The oxidation of BC (either by biological aging in soil or after chemical treatment) will decrease its potential to donate electrons and support N_2O reduction by *P. denitrificans*.

MATERIALS AND METHODS

BCs

A total of nine BCs were tested stemming from a variety of feedstocks (Table 1). A total of six BCs were produced from tree-plant residues pyrolyzed at two different temperatures. More information about their origin can be found in Sánchez-García *et al.* (2019). A company (PROININSO, S.A. Málaga, SPAIN) supplied another woody BC (oak trees). This BC was used (i) fresh, as commercially acquired and (ii) aged (Table 1), after 5 years in a soil field experiment (Sánchez-García *et al.* 2016). This aged BC was recovered by collecting the particles by hand from the field, followed by several milliQ water washes. Lastly, a modified BC from olive trees was synthesized by a post-pyrolysis chemical treatment (Lima *et al.* 2017). Briefly, the char was subjected to a series of oxidative steps using $NaNO_3$, H_2SO_4, $KMnO_4$ and

Table 1. Feedstock, pyrolysis temperature and some of the most relevant physicochemical properties of the BCs used at the incubations.

Feedstock	BC-Olv400 Olive tree	BC-Olv600	BC-OlvM*	BC-To400 Tomato plants	BC-To600	BC-Ri400 Rice straw	BC-Ri600	BC-Oak650 Holm oak tree	BC-Oak650A**
T pyrolysis (°C)	400	600	400	400	600	400	600	650	650
pH	9.90	11.05	8.0	9.65	12.10	9.73	10.21	9.4	7.1
EC (mS cm^{-1})	0.59	0.75	0.25	18.43	22.80	3.83	4.43	0.40	0.97
Ash (%)	4.9	4.8	16	34.4	38.2	36.6	41.9	13	12
C (%)	59.7	57.7	63.2	21.0	21.3	32.8	31.6	66.8	65.3
N (%)	0.84	0.93	0.71	2.12	1.92	0.66	0.58	0.70	0.91
O (%)	18.2	12.9	16.7	53.5	53.1	49.4	50.1	31.1	32.2
H (%)	0.84	1.73	3.32	2.78	1.23	2.39	1.22	1.40	1.59
Atomic H/C	0.13	0.25	0.47	0.80	0.34	0.60	0.30	0.25	0.29
Atomic O/C	0.18	0.11	0.15	0.96	0.91	0.78	0.78	0.35	0.37
C/N	107.5	106.0	103.3	22.9	26.9	95.6	96.9	111.2	83.7
Lig/cell (feedstock)	0.46	0.46	0.46	0.30	0.30	0.42	0.42	0.70	0.70

*Chemically modified BC-Olv400 post-pyrolysis; **Weathered BC-Oak650. EC: electric conductivity; lig/cell: ratio lignin/cellulose of BCs feedstock (Sánchez-García *et al.* 2019).

H_2O_2. The objective of synthetizing this BC was to obtain a BC with greater electron exchange capacity by increasing the number of surface redox-active functional groups. Stock suspensions of all BCs were prepared by adding 10 g of BC powder to 100 mL of anoxic milliQ water inside a glovebox (MBraun UniLab-2000, Germany). The suspensions were sonicated for 10 min and sterilized in an autoclave (Kappler *et al.* 2014; Yang *et al.* 2020).

BC characterization

A detailed characterization of BC-Olv400, BC-Olv600, BC-To400, BC-To600, BC-Ri400 and BC-Ri600 can be found in Sánchez-García *et al.* (2019) and a summary in Table 1. The characterization of the other BCs used is provided in Tables S1, S2 and Figure S1 (Supporting Information). Additionally, the Brunauer–Emmett–Teller (BET) surface area (m^2/g BC) was analyzed (ASAP 2000 instrument, Micromeritics, Norcross GE, USA). The BCs' electron donating capacity (EDC) and electron accepting capacity (EAC) were determined for the BC suspensions by mediated electrochemical reduction and oxidation (1000C Multi-potentiostat, CH Instruments, Austin TX, USA) using the electron transfer mediators 4,4'-bipyridinium-1,1-bis(2-ethylsulfonate) (*ZiV*) and 2,2,'-azino-bis(3-ethylbenzothiazoline-6-sulfonic acid) diammonium salt (ABTS), respectively. The resulting reductive (MER) and oxidative (MEO) current peaks were integrated to yield EAC and EDC (mmol/e$^-$/g BC) (Klüpfel *et al.* 2014)

$$E\,AC = \frac{\int I_{red}/F\,dt}{m_{BC}} \; ; \; E\,DC = \frac{\int I_{ox}/F\,dt}{m_{BC}} .$$

In these equations, the reductive and oxidative baseline-corrected currents in MER and MEO are represented by I_{red} and I_{ox} respectively, F is the Faraday constant (96 485.34 s A mol/e$^-$) and m_{BC} is the added mass (g) of biochar (BC).

Microorganism used and cultivation conditions

Paracoccus denitrificans ATCC 19 367 (provided by Sebastian Kopf, California Institute of Technology) was used as a typical denitrifying bacterium. The culture medium was prepared with 22 mM NaHCO$_3$ buffer (adjusted to pH 7) with all the compounds listed in Table S3 (Supporting Information). This culture medium was divided into flasks containing 25 mL of each of them. To each of
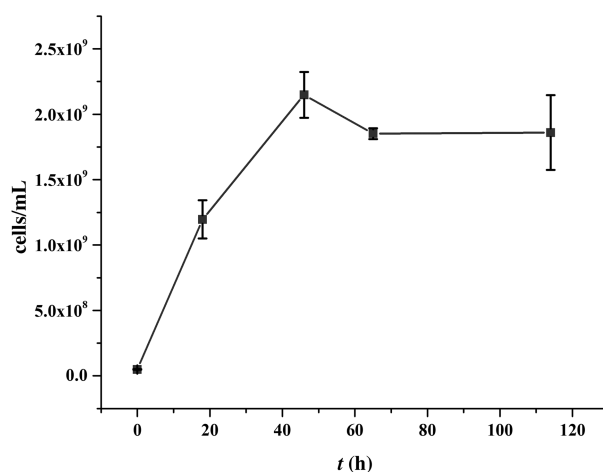
Figure 1. Growth of *P. denitrificans* ATCC 19 367 when incubated with the substrates shown in Table S3 (Supporting Information). The incubation was done for 120 h in the dark at 28°C.

these 25 mL-flasks, the following were added: a 1.25 mL aliquot from the initial stock of *P. denitrificans* ATCC 19 367 with 3.6×10^7 cells/mL, 500 μL of the electron donor NaNO$_3$ (1 M) and 250 μL of the electron acceptor succinate (1 M). The cultures were incubated anoxically in the dark at 28°C without any shaking.

During pre-cultivation, *P. denitrificans* growth was followed by quantifying cell numbers every day for five days with a Flow Cytometer (Attune *NxT* acoustic focusing cytometer and auto sampler, Life technologies. ThermoFisher Scientific, Santa Clara CA, USA) using a commercial LIVE/DEAD BacLight Bacterial Viability Kit (Molecular Probes. L-7012). Its growth rate is shown in Fig. 1 (final cell number: 2.15×10^9 cells/mL).

N$_2$O reduction setups

A succession of vacuum and N$_2$ flushes were applied to 58 mL serum bottles (HCl-washed and sterilized by autoclaving). Afterwards, anoxic conditions were established by filling the bottle with a mixture of N$_2$/CO$_2$ (80/20 %vol). A total of twenty mL of NaHCO$_3$ (22 mM) buffer solution were added to each bottle as well as the required volumes of the 0.1 g/mL suspensions of the BCs. A total of 36 different treatments were set up depending on the BCs, their concentrations, 1 (BC1) and 5 (BC5) g/L and the

conditions, abiotic (A) or biotic (B). In addition, two controls were prepared, BC0_A and BC0_B, both of them with 0 g/L of BC. In case of the biotic samples, *P. denitrificans* ATCC 19 367 cells were injected (750 μL of the initial stock (previous section) at an initial cell number of 1.1×10^6 cells/mL). Lastly, $NaHCO_3$ (22 mM) was used for equating the volumes to 25 mL and the resulting overpressure was released. No electron donor or acceptor aside from BC was added. After two days of equilibration (at which the small residual $NaNO_3$ and succinate that could have remained from the growth culture was assumed to be consumed), 0.6 mL of sterilized N_2O (99%) were injected into the headspace (initial N_2O concentration around 2.3% vol) after which the overpressure was released. Gas samples were taken for 1 week from the bottles at regular intervals. Throughout the entire procedure, the pureness of the culture inside the samples jars was ensured by operating close to a Bunsen burner, using sterilized material and employing 90% ethanol constantly. The incubations were carried out in the dark, at 28°C and on a shaker at 100 Mot 1/min (Edmund Bühler GmbH SM-30C, Germany).

The nomenclature for the different treatments was as follows: BCX_YT_Z, where X indicates the concentration of BC (0, 1 or 5 g/L), Y stands for the original feedstock (Olv, To, Ri, Oak), T denotes the highest temperature of pyrolysis (400, 600 or 650°C) and Z the biotic (B) or abiotic (A) nature of the experiment. For the aged and modified BCs, an extra letter was added after the one referring to the feedstock, A and M respectively (BCX_Oak650A_Z, BCX_OlvM_Z)

Nitrous oxide measurements

Gas samples of 100 μL were taken using a gastight syringe and transferred into N_2-filled 22.4 mL glass vials. Nitrous oxide concentrations were determined using a gas chromatograph (GC 450 Greenhouse Gas Analyzer, Bruker Daltonic, Bremen, Germany) coupled to an autosampler (GX-271 LH, Gilson, Limburg, Germany). The separation of the trace gases was carried out using a Hayesep D column (80–10 mesh), with the oven temperature set at 80°C. N_2O concentration was analyzed with a ^{63}Ni electron capture detector at 300°C, which employs N_2 as the carrier gas and a mixture of 90% argon and 10% methane as the makeup gas. Standard gases with 25, 50, 75 and 100 ppm N_2O in N_2 were used for calibration (nonlinear). Chromatograms were integrated using Bruker Compass CDSTM 2012 software.

EDC evolution measurements

Samples volumes of 500 μL were taken from each bottle at the beginning (before the N_2O injection) and at the end of the experiment (162 h after the N_2O injection). Sampling was carried out inside a glovebox where the aliquots were centrifuged for 5 min at 20 000 x *g* and washed with anoxic milliQ H_2O until reaching a neutral pH (this step was not necessary in our case as every sample was already at pH 7). Afterwards, 1 mL anoxic milliQ H_2O was added to each sample and, additionally, those with 5 g/L of BC were diluted 1:5. After being thoroughly shaken with a Vortex, every sample was immediately frozen at −20°C until measured. EDC determinations were performed electrochemically as described previously (Klüpfel *et al.* 2014).

Qualitative microscopy assays

The bacteria–biochar attachment was analyzed by fluorescence microscopy (Leica DM 5500B, Leica, Germany). The living cells were visualized at 488 nm in green after being stained by DNA dye Syto 9 combined with propidium iodide (LIVE/DEAD BacLight Bacterial Viability Kits, Molecular Probes. L-7007).

Calculations and statistical analyses

Biochar redox characteristics, EDC and EAC, were calculated in duplicate as described by Klüpfel *et al.* (2014). The electron exchange capacity, which describes a BC total capacity to donate and accept electrons, was obtained by adding the value of EDC to EAC (EEC = EAC + EDC). In addition, the EDC/EEC ratio or reduction index (RI) of the BCs was determined, which is a direct measurement of its relative extent of reduction (or oxidation; Klüpfel *et al.* 2014).

The N_2O concentration at time = n hours ($[N_2O]_n$ in mg N-N_2O/flask) was plotted normalized in respect with the concentration at time 0 h ($[N_2O]_0$) for facilitating the comparison between treatments. It was represented as $^C/_{C_0}$ and calculated:

$$^C/_{C_0} = [N_2O]_n / [N_2O]_0$$

Soil reduction of N_2O and formation of N_2 follows a competitive Michaelis–Menten type kinetics but can be simplified to first order kinetics at low nitrate concentrations (Van Cleempt *et al.* 1975; Cho and Mills 1979). Values of $^C/_{C_0}$ against time was calculated (for the first 45 h of incubation) and the data fitted to a straight line with slope k and intercept a.

$$t = k \cdot {}^C/_{C_0} + a$$

As a way to assess the rate of change in the N_2O concentration with time, the 'N_2O reduction extent' was defined as:

$$N_2O \ reduction \ extent = ([N_2O]_0 - [N_2O]_n) \ x \ 100$$

To estimate the differences among treatments, the standard deviation was calculated from triplicate or duplicate replicates. Additionally, when possible, the significant differences were determined by a one-way ANOVA. The Tukey's post hoc test ($P < 0.05$) was used to discriminate treatments within groups. For significant differences, different letters were assigned. Additionally, an electron balance was performed by calculating the number of electrons needed for the N_2O reduction observed from the start to the end of the incubations (165 h). For these calculations, both the N_2O in the headspace and the one dissolved were considered, for which the N_2O solubility at 28°C (4.032×10^{-4}) and its Ostwald Coefficient (0.5553) were used (Wilhelm, Batting and Wilcock 1977). A Hierarchical Cluster Analysis was carried out to group the treatments as a function of BCs RI and the N_2O reduction extent they produced considering the whole period of incubation ($n = 162$ h in the above equation) . The Ward method was applied with the aim of grouping cases so as to minimize the variance within clusters.

A Principal Component Regression (PCR) was also performed. A dimension reduction with Oblim rotation was applied over a selection of BC properties. It resulted in a number of principal components arranged in a matrix and composed by positive and negative coefficients assigned to each BC property. Values lower than +0.52 or −0.52 were not considered and deleted from the matrix. Afterwards, a linear regression was carried out with the mentioned matrix as the independent factor and the N_2O reduction extent (*t* 0 to *t* 165 h) for the biotic samples with BC 5 g/L as the dependent factor. The higher the coefficient assigned to

a certain BC property in the matrix, the stronger the influence it has over the dependent variable. Those negative values will have an inverse relation with dependent value whereas positive numbers will indicate a direct relation.

All the mentioned statistical analyses were developed with IBM SPSS Statistics v.23 and every graph included was drawn with Origin 2018 64Bit software.

RESULTS AND DISCUSSION

BC characterization

The quantification of BC redox properties is depicted in Fig. 2. The EDC values were lower for BCs pyrolyzed at 600°C as compared to 400°C while the trend for the EAC was exactly the contrary. This is in agreement with previous studies (Klüpfel *et al.* 2014; Prévoteau *et al.* 2016; Zhang *et al.* 2018). Biochars generated at intermediate temperatures (300–400°C) preferentially function as electron donors due to the presence of surface functional groups, as their amorphous carbon structure limits electron transport (Klüpfel *et al.* 2014; Sun *et al.* 2017). In contrast, BCs with a high proportion of graphitic structures (high HTT BCs) donate fewer electrons due to a lower content of hydroxyl groups induced by the dehydration of lignin-derived phenols and alcohols, coupled with the onset of aromatization while the temperature rises (Harvey *et al.* 2012).

The post-pyrolysis oxidation treatment applied to BC-Olv400 largely increased both the EDC and EAC of BC-OlvM by creating additional redox-active functional groups (Lima *et al.* 2017). This increment was especially substantial for the EAC, which was nearly 15 times (5.81 mmol of e^-/g BC) the one of BC-Olv400 (0.39 mmol of e^-/g BC). The slight increase in the EAC of BC-Oak650A in comparison to BC-Oak650 reflects the oxidation processes related to aging in soil. These processes affect BC surface and redox properties due to the formation of heterogeneous coatings (Cheng *et al.* 2006; Wiedner *et al.* 2015; Archanjo *et al.* 2017; Hagemann *et al.* 2017) by precipitation of organic molecules and inorganic mineral compounds (Prévoteau *et al.* 2016).

The reduction index (RI), varies widely for our BCs (Fig. 2), with values ranging from 0.17 (the most oxidized BC, BC-OlvM) to 0.77 (the most reduced BC, BC-To400). Without taking into consideration other parameters, based on our hypothesis and on these RI values, those BCs that would promote the microbial reduction of N_2O concentration to a greater extent would be (from the strongest reducer to the least): BC-To400 > BC-Ri400 > BC-Olv400 > BC-To600 > BC-Ri600 > BC-Olv600 > BC-Oak650 > BC-Oak650A > BC-OlvM.

All BCs generally exhibited low surfaces areas (Fig. 3), with values ranging from 1.16 to 20 m^2/g, with the exception of BC-Oak650 (175.2 m^2/g). A clear trend in relation to BCs pyrolysis temperature was not observed. After the bio-physico-chemical weathering in soil for four years, the BET surface area of BC-Oak650 decreased, significantly but was still the BC with the second highest BET value. A decrease of surface area of BC after aging has been previously documented and has been related to pore clogging by the formation of heterogeneous coatings consisting of different mineral compounds associated with organic compounds (Archanjo *et al.* 2017).

Microbial nitrous oxide reduction

The evolution of N_2O in the biotic treatments over incubation time is shown in Fig. 4. Its concentration decreased significantly for the majority of the BC-amended treatments. In some cases, N_2O was even completely removed (BC5_Ol400_B and BC5_To400_B) or diminished to a final concentration of 7.2% of the initial value (BC5_Ri400_B). Nevertheless, when the bacterium was in contact with N_2O without the presence of any BC (BC0_B, Fig. 4) or with BC-OlvM, nearly no change in its concentration was detected. A very similar pattern was observed for abiotic samples (Figure S2, Supporting Information), in which C/C_0 did not vary more than 20%. These results suggest that the BCs promote microbiological N_2O reduction (as part of the denitrification pathway).

Nonetheless, it was observed that especially for samples BC1_Oak_B, BC5_Oak_B, BC5_OakA_B or some abiotic setups (e.g. BC1_Ri400_A), there was a slight increase in the N_2O concentration. Although no N source was been added to the sample flasks, these minor increases could have been attributed to N_2O production by *P. denitrificans* with either the remaining electron donor $NaNO_3$ used for bacterial growth or some nitrogen component in BC. The ability of *P. denitrificans* to generate N_2O is well known (Gaimster *et al.* 2018). However, under an anoxic atmosphere and NO_3^--limited conditions, its major denitrification product is N_2 (Felgate *et al.* 2012). Hence, as the increase of N_2O content in the flasks is not steady but fluctuating and the mentioned BC causing these increments are the ones with greater BET surface areas (Fig. 3), we speculate that adsorption-desorption mechanisms might be responsible for this fluctuation in N_2O concentration . Although research studies focusing on BC potential to adsorb N_2O in solution were not found, some experiments have proved that preparations of anhydrous BC sorbs up to 2–16 mg N_2O per g BC (Cornelissen *et al.* 2013). In addition, under high levels of moisture (75%, water holding capacity, WHC), it was demonstrated that BC is able to absorb and transport CH_4 (Sadasivam and Reddy 2015). The reason why samples BC1_OlvM_A and BC5_OlvM_A (Figure S2, Supporting Information) produced a slight reduction of N_2O in spite of having a very low BET surface area (Fig. 3), is currently unknown.

The change of BC concentration from 1 to 5 g/L had a substantial impact for the N_2O reduction observed across the biotic incubations if the results of the first 45 h of incubation are considered. During this period, most decreases in N_2O occurred in our incubations (Fig. 4) and the major denitrification activity of *P. denitrificans* takes place (Baumann *et al.* 1996). Table S4 (Supporting Information) shows the slope and R^2 of the fitting lines that resulted from adjusting the decrease of N_2O during the period mentioned to a straight line. In addition, the relation of slopes at both BC concentrations is included (k5/k1). It is clearly noticeable that this decrease is more pronounced with 5 g/L BC than with 1 g/L BC. At the lowest BC concentration, only BC1_Ri600_B and BC1_To400_B slopes differed significantly from the rest of the treatments. Whereas, at the highest concentration (5 g/L), significant differences were observed between the control and every BC pyrolyzed at 400°C as well as BC5_Ri600_B. The extent of the change (k5/k1) varied depending on the BC. The greatest shift was achieved by BC-Oak650 and BC-Ri400 (5.4 and 4.6, respectively). Only BC-Oak650A and BC-OlvM k5/k1 were close to zero, and these were precisely the BCs showing nearly no reduction of N_2O (Fig. 4). Increasing effects following an increment in the dose of BC have been previously detected in other BC experiments (Kappler *et al.* 2014; Weldon *et al.* 2019).

To ascertain if a relationship existed between the evolution of the N_2O concentration caused by the BC and their redox potential, the BC's t reduction index (RI) was plotted against the extent of N_2O reduction (% of $[N_2O]_0$-$[N_2O]_{162}$ for the biotic samples with 5 g/L BC), which results are shown in Fig. 5. All BCs
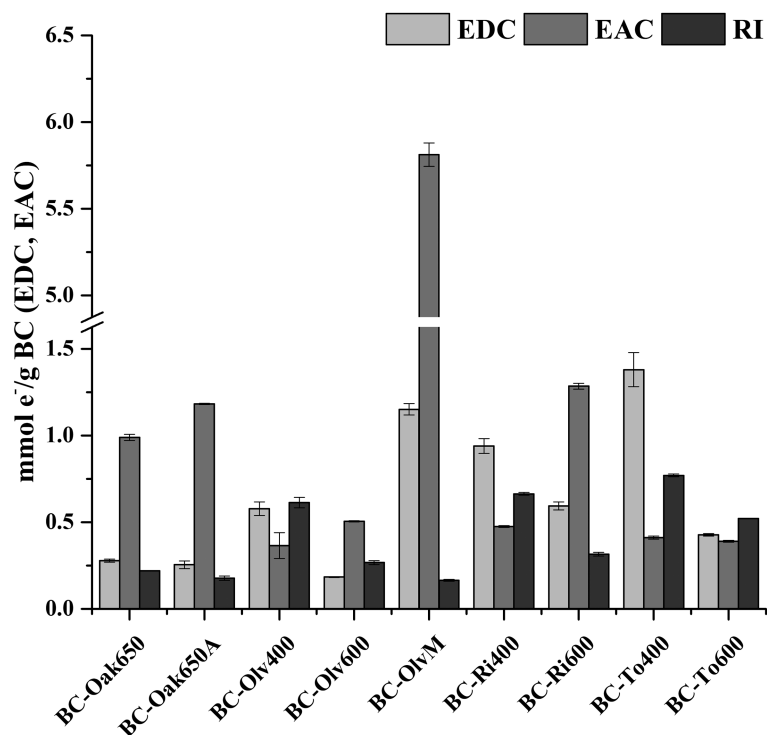
Figure 2. Electron donating capacity (EDC), electron accepting capacity (EAC) (mmol e⁻/g BC) and reduction index (RI, i.e. EDC/EEC) measured in BC suspensions of 10 g/100 mL.
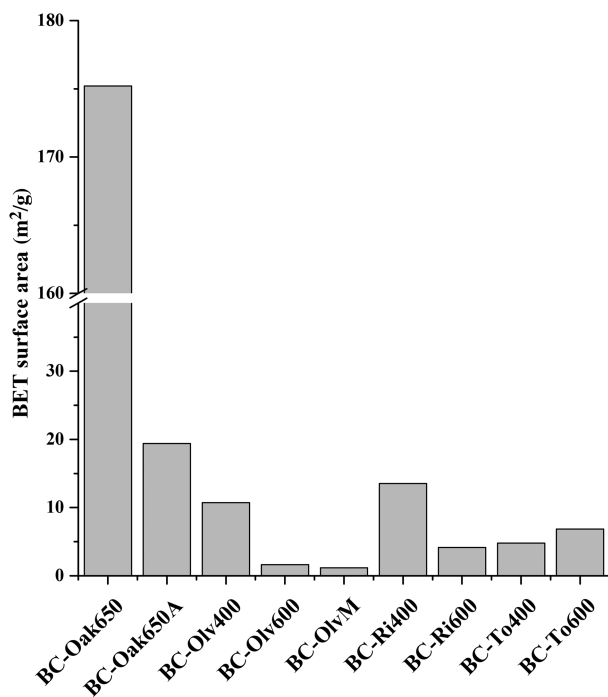

Figure 3. Brunauer–Emmett–Teller surface area (BET; m^2/g) of all BCs used at the incubations.

pyrolyzed at 600°C showed less than 45% removal of N$_2$O and no more than a 50% change of RI, whereas the BCs pyrolyzed at 400°C showed higher values of both (>65%). The only exception to this rule was BC-Ri600, which showed one of the highest N$_2$O

reduction extents (100%) for its modest RI (31.6%). The Hierarchical Cluster Analysis applied confirmed the two groups separated in Fig. 5 are statistically different (ANOVA F value = 34.676; Prob>F = 3.822 10^{-6}): one composed by all BCs pyrolyzed at 600–650°C together with BC-OlvM and the other by BCs produced at 400°C plus BC-Ri600.

Chen *et al.* (2018) studied in detail which redox-active compounds of BC contributed to N$_2$O reduction in an experiment with denitrifying bacteria. They concluded that BC enhances denitrification through different mechanisms depending on its temperature of production. Biochar produced at low temperatures will enhance the process through its role as electron donor, and BC created at high temperatures through its ability to accept electrons together with its electrical conductive structure. This is in agreement with what we obtained in Fig. 5: the mechanism through which the tested BC promoted a greater extent of N$_2$O reduction (all the ones pyrolyzed at 400°C) would mainly be thanks to their potential to donate electrons (specifically their RI), which confirms our first hypothesis. However, the non-perfect adjustment of the fitting line depicted in Fig. 5 (R^2 = 0.5811), together with the fact that samples with BC-Ri600 produced a high N$_2$O reduction with no connection to its RI, suggest that other factors exist aside from the BCs' redox properties that could be involved and that actively determine the outcome of the incubation.

This hypothesis is supported by the position of the chemically-modified BC (BC-OlvM) at the bottom left of the graph in Fig. 5. It seems to demonstrate that an extraordinary enhancement on both EAC and EDC is counter-productive if it results in a low RI. Moreover, it might show that having an ordered and condensed aromatic structure is necessary. The harsh chemical oxidation procedure applied to BC-OlvM (which was initially also produced at 400°C) consumed reducing equivalents (electrons) from its structure (Lima *et al.*
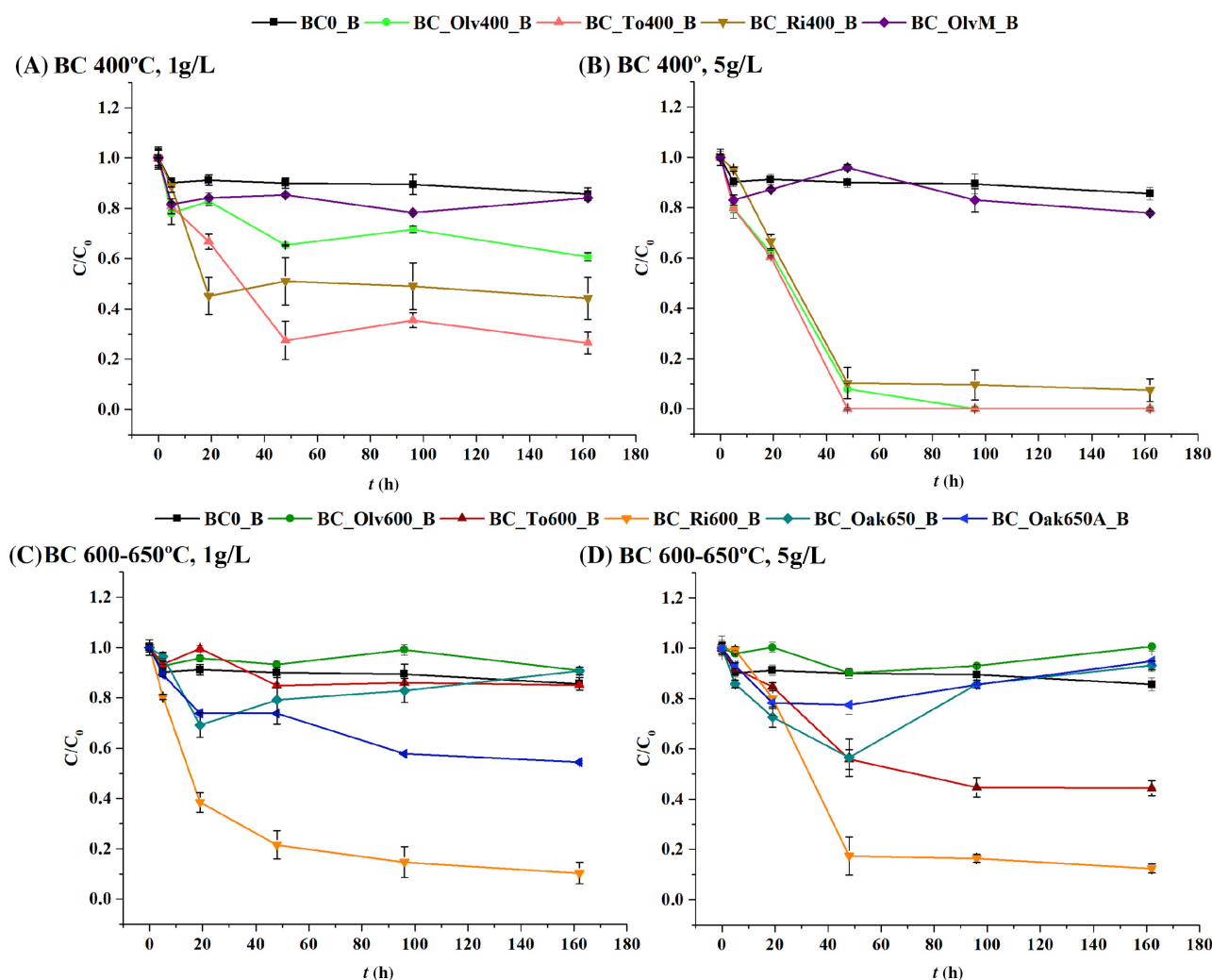
Figure 4. Change in relative N₂O concentrations shown as C/C₀, where C refers to the N₂O concentration (mg N in N₂O) per bottle at a specific time point and C₀ refers to the N₂O concentration at time 0. All samples contained *Paracoccus denitrificans* (biotic samples). Setups (a)–(d) vary regarding BC concentration and temperature of BC pyrolysis.

2017). Therefore, this ability of BC to donate electrons was decreased by a near-complete destruction of its prevailing aromatic ring structures and chemical functional groups (Chacón *et al.* 2017). Furthermore, BC-OlvM had a very high concentration of Mn (88 157 ppm, Table S2, Supporting Information) that could potentially be toxic to the bacteria (Kaur *et al.* 2017). Consequently, the basis of our second hypothesis 'the oxidation of BC will decrease its potential to donate electrons and support N₂O reduction by *P. denitrificans*' has been demonstrated, although the reasons are much more intricate, as explained above.

Biochar BC-Oak650 and its weathered variant BC-Oak650A showed a very similar behavior in the N₂O reduction assays leading to a modest microbial reduction of N₂O. This suggests that 5ars of field ageing did not decrease the ability of BC to stimulate the reduction of N₂O by *P. denitrificans*. At a concentration of 1 g/L, the BC-Oak650A even resulted in N₂O reduction that was four times higher as compared to the fresh BC, resulting in the rejection of part of our second hypothesis: soil ageing would decrease BC's ability to support microbial N₂O reduction. Nevertheless, our findings agree with the results by Hagemann *et al.* (2017).

In their research, a BC placed in soil for three years was shown to have the same potential to reduce N₂O emission in comparison with its fresh version. They attributed this activity to a combination of processes that take place during BC ageing, including its breaking down into smaller particles, higher amounts of oxidized functional groups on its surface, and a lower pH. We observed that during ageing of BC-Oak650A, its EAC slightly increased while its pH, BET surface area and C/N ratio decreased substantially in comparison with BC-Oak650 (Fig. 2, Table 1 and Table S1, Supporting Information). Our study showed substantial differences between field-aged BCs and chemically-oxidized BCs; whereas field aging did not affect N₂O reduction significantly, chemical oxidation invalidated the effect of BC-Olv400. During soil weathering, BC undergoes a wide range of physical and chemical transformations that differ from those obtained by chemical treatments (such as our modified BC (BC-OlvM) or H₂O₂-treated BCs (Yuan *et al.* 2019). Therefore, caution needs to be taken when extrapolating the results from chemically-altered BCs to aged BCs. In summary, we have proved that BC soil weathering would not necessarily imply a decrease in its ability to
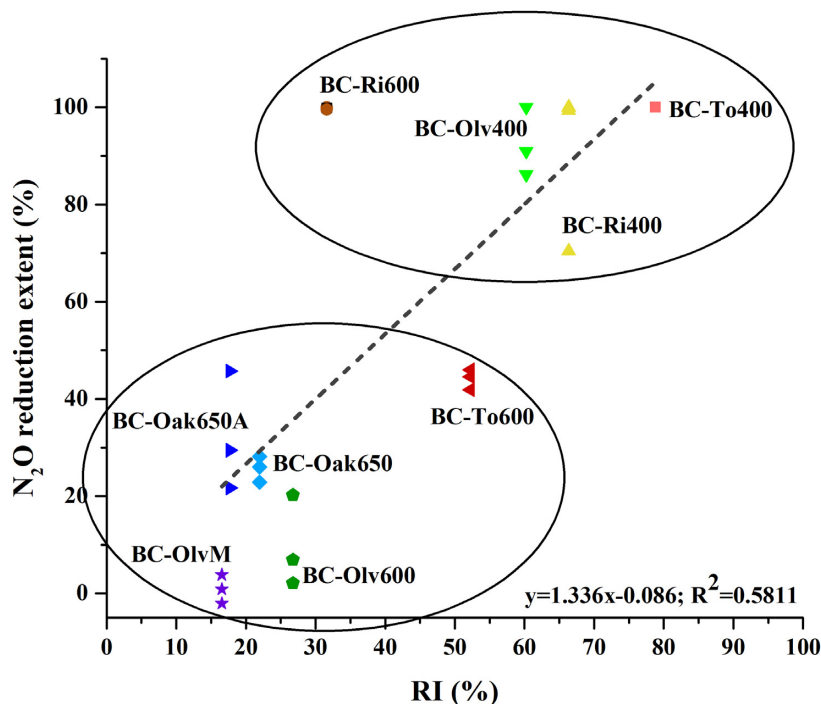
Figure 5. Correlation between the microbial N_2O reduction (% of initial N_2O reduced after 162 h) versus BCs RI. The values of the extent of N_2O reduction were calculated for biotic setups with a BC concentration of 5 g/L. The data was adjusted to a line which equation and R^2 appears at the bottom right corner of the graph (Pearson's r = 0.7623, ANOVA F value = 34.676, Prob>F = 3.822 $\times 10^{-6}$). The two groups marked with circles are the result of the application of the Hierarchical cluster analysis.

reduce N_2O to N_2. A mix of factors could be involved, as BC-Oak650A and BC-Oak650 had nearly the same incubation outcome, having similar redox properties but substantially differing in other characteristics.

Change of BCs redox state and electron balance

In addition to changes in N_2O concentration during the incubations in the presence/absence of *P. denitrificans*, we also followed the changes of the BCs' EDC values. The measurements were made at the beginning of the experiment, before N_2O was injected into the headspace and at the end of the incubation, after 162 h. Table S5 (Supporting Information) summarizes these results for samples with BC 5 g/L under biotic and abiotic conditions. In addition, it shows the theoretical amount of e^- required to explain the observed decrease in N_2O concentration during that period (0–162 h). Unfortunately, the EDC values did not show any significant differences among treatments due to the variability in the replicates. In addition, the electron balance for the biotic samples showed that only BC-Olv600, BC-To400, BC-Oak650 and BC-Oak650A provided enough electrons for the reduction of N_2O undergone in their samples. As shown previously (Fig. 5), the RI (EDC/EEC) of the BC is directly correlated to N_2O reduction by *P. denitrificans*, but not the EDC of the BC. Hence, not having measured the changes in EAC throughout the incubation period may be one of the reasons why we cannot see a correct balance of electrons. The influence of other BC characteristics, which may be affecting this outcome, needs to be considered as well. In addition, we do not discard *P. denitrificans*' stored C as being an extra source of electrons, a process that has been proven to occur for other bacteria (Jiang and Kappler 2008). This variability on the connection between the mmol e^- needed for N_2O reduction and the ones missing in the BCs is showcased by the representation of Table S5 (Supporting Information) with

replicates (n = 3) in Fig. 6. Nevertheless, what this figure demonstrates is what it was also observed in Figure S2 (Supporting Information): the underlying process driving N_2O reduction was mostly biotic.

Support for microbiological N_2O reduction in connection with BC also comes from microscopic analyses. Microscopy images taken at the end of the incubations (Figure S3, Supporting Information) showed that most bacterial cells were associated with BC particles. Although further conclusive analyses or techniques would be needed, these observations do not rule out the possibility that BC indeed serves as an electron donor for N_2O reduction by *P. denitrificans*. This process of electron donation by BC for N_2O reduction does not require the formation of conductive structures such as pili. Instead, it seems sufficient for the cells to be tightly attached to the BC (Chen *et al.* 2014; Yu *et al.* 2016; Baek *et al.* 2018; Zhang *et al.* 2018).

Correlation of BC properties with N_2O reduction by *P. denitrificans*

To further investigate the potential role of BC redox properties and to elucidate which others could significantly influence N_2O reduction, a Principal Component Regression (PCR) was carried out for the samples containing 5 g/L BC. From the wide range of BC's physical and chemical characteristics that were subjected to the PCR, the ten included in Table 2 were selected for being the most relevant. The reduction of variables applied separated them into three components (Bartlett's Sphericity test significance P-value = $p < 0.05$). The linear regression results showed component 1 and 3 as being relevant to a strong extent of N_2O reduction with a combined value of 56.0% (21.5 and 34.5%, respectively). Therefore, it is confirmed that the redox properties of BC (EAC, EDC and RI) have a substantial influence over *P. denitrificans* N_2O reduction. High values of EDC (coefficient of +0.895)
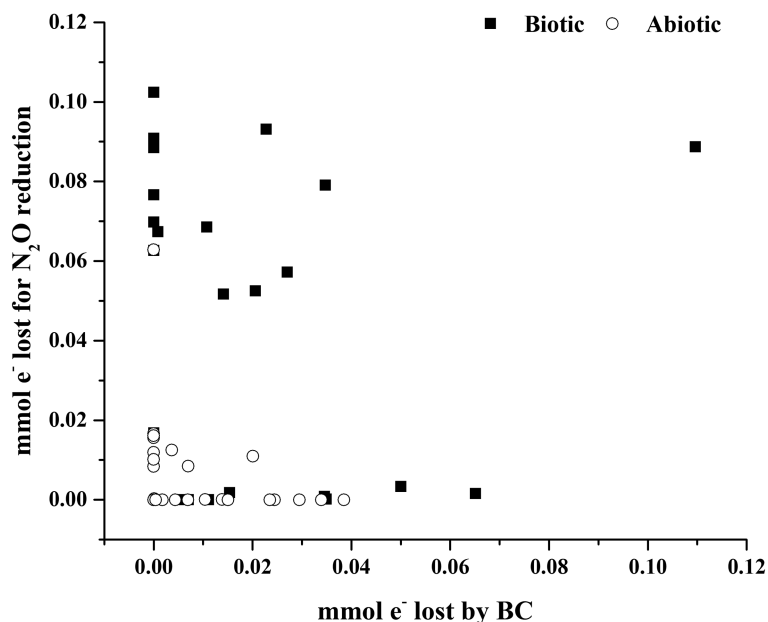
Figure 6. Amount of electrons (mmol e⁻/flask) needed for the decrease in the N_2O concentration throughout the incubation period (162 h) versus the electrons lost by BC. Filled black squares represent the biotic samples and the open circles the abiotic ones, both including every BC treatment (5 g/L) sample with their triplicates.

Table 2. Principal Component Regression (PCR) matrix and outcome. The 3-component rotation matrix is shown into which the BC characteristics were ordered. The coefficients for each of them were sorted according to value and the ones < 0.52 were deleted. The result of the contribution of the components to the observed extent of N_2O reduction (in % for the biotic samples with BC 5 g/L) analyzed by a linear regression, were included on the bottom of the table (R^2, ANOVA F and Sig. ANOVA).

	Component		
	1	2	3
EAC	−0.937		
Lig/cell	−0.918		
BET	−0.801		
Ash	0.529		
Fe		0.962	
C/N		−0.931	
EC		0.780	
EDC			0.895
H/C			0.885
RI			0.729
Variance explained (%)	45.7	26.5	16.0
R^2	0.215	-	0.345
ANOVA F	18.45	-	15.82
Sig. ANOVA	0.000	-	0.000

EAC: electron accepting capacity; Lig/cell: proportion of lignin and cellulose in the feedstock; BET: Brunauer−Emmett−Teller surface area; EC: electric conductivity; EDC: electron donor capacity; RI: reduction index; ANOVA F: value of F; Sig. ANOVA: F statistical significance.

and RI (+0.729) together with low values of EAC (−0.937) favor a strong extent of N_2O reduction. In addition, a low proportion of lignin over cellulose (lig/cell) on the feedstock, a lower BET surface area and a high H/C and ash content affected the reduction of N_2O by *Paracoccus denitrifcans*.

The H/C ratio is regarded as an indicator of the BCs' aromatic index, i.e. aromatic structures that have been found to increase BC's redox activity (Klüpfel *et al.* 2014; Yuan *et al.* 2017).

High values of H/C are generally found in BCs produced at low temperatures (Suliman *et al.* 2016; Sánchez-García *et al.* 2019). Moreover, the proportion of lignin and cellulose on the feedstock determine, to a great extent, the amount and nature of electron-accepting and donating moieties found on BC (Prévoteau *et al.* 2016). The PCR outcome suggests a low-lignin biomass, thus no woody materials, would be more appropriate for BC feedstock in order to assist *P. denitrificans'* N_2O reduction. The BC surface area is an indicator of its capacity to absorb molecules as gases (Lehmann and Joseph 2009) and is inversely related with its ash content (Ronsse *et al.* 2013). Both their appearance with negative and positive coefficients, respectively, in Table 2, suggest that the abiotic process of N_2O absorption is not a major mechanism under our experimental conditions.

Therefore, without taking into consideration the redox properties, this statistical analysis points out that straw and crop residues (i.e. BC-Ri and BC-To) pyrolyzed at low temperatures (400°C) had the greatest number of the characteristics needed to achieve a greater and more efficient N_2O reduction by *P. denitrificans* than BCs produced from wood pruning (BC-Olv and BC-Oak). However, comparing BCs is very intricate, due to the high variability of their physical and chemical characteristics, and the complexity increases when linking these properties to their production feedstock and effects, suggested to be independent (Ronsse *et al.* 2013) and antagonistic (Weldon *et al.* 2019), respectively.

CONCLUSIONS

Our results demonstrate that BC aids *P. denitrificans*, facilitating the reduction of N_2O to N_2, mainly by means of its reduction state. Nevertheless, the extent of this reduction is significantly affected by other BC physical and chemical properties, in particular those ruled by their feedstock and pyrolysis temperature. For this specific BCs series, we found that BCs produced at a low temperature (400°C) and coming from non-woody biomass (high H/C and ash percentage together with low surface area and poor lignin feedstock content) promoted larger extent of N_2O

reduction in the presence of *P. denitrificans*. In addition, we have proved the biotic character of the process, as no N_2O reduction was achieved in the absence of the bacterium. This study provides information for generating on demand and tailor-made BCs with the specific mentioned goal in mind. However, research in this field is still at an early stage, and further research is needed. More specifically, isotopic experiments and molecular biology analysis of DNA and RNA focused on the expression of the functional genes encoding the reduction of N_2O to N_2, would be important. Additionally, incubation experiments including an electron donor/acceptor aside from BC would be essential to prove the role and extent of the latter to support N_2O reduction in laboratory set-ups that closely mimic natural soil conditions.

SUPPLEMENTARY DATA

Supplementary data are available at FEMSEC online.

REFERENCES

Archanjo BS, Mendoza ME, Albu M *et al*. Nanoscale analyses of the surface structure and composition of biochars extracted from field trials or after co-composting using advanced analytical electron microscopy. *Geoderma* 2017;**294**:70–9.

Baek G, Kim J, Kim J *et al*. Role and potential of direct interspecies electron transfer in anaerobic digestion (review). *Energies* 2018;**11**:107.

Baumann B, Snozzi M, Zehnder AJB *et al*. Dynamics of denitrification activity of *Paracoccus denitrificans* in continuous culture during aerobic-anaerobic changes. *J Bacteriol* 1996;**178**:4367–74.

Borchard N, Schirrmann M, Cayuela ML *et al*. Biochar, soil and land-use interactions that reduce nitrate leaching and N_2O emissions: a meta-analysis. *Sci Total Environ* 2019;**651**:2354–64.

Butterbach-Bahl K, Baggs EM, Dannenmann M *et al*. Nitrous oxide emissions from soils: how well do we understand the processes and their controls? *Phil Trans R Soc* 2013;**B368**:20130122.

Carreira C, Pauleta SR, Moura I. The catalytic cycle of nitrous oxide reductase- the enzyme that catalyzes the last step of denitrification. *J Inorg Biochem* 2017;**177**:423–34.

Cayuela ML, Sánchez-Monedero MA, Roig A *et al*. Biochar and denitrification in soils: when, how much and why does biochar reduce N_2O emissions? *Sci Rep* 2013;**3**:1–7.

Cayuela ML, Van Zwieten L, Singh BP *et al*. Biochar's role in mitigating soil nitrous oxide emissions: a review and meta-analysis. *Agr Ecosyst Environ* 2014;**191**:5–16.

Chacón FJ, Cayuela ML, Roig A *et al*. Understanding, measuring and tuning the electrochemical properties of biochar for environmental applications. *Rev Environ Sci Biotechnol* 2017;**16**:695–715.

Chen G, Zhang Z, Zhang Z *et al*. Redox-active reactions in denitrification provided by biochars pyrolyzed at different temperatures. *Sci Total Environ* 2018;**615**:1547–56.

Cheng CH, Lehmann J, Thies JE *et al*. Oxidation of black carbon by biotic and abiotic processes. *Org Geochem* 2006;**37**:1477–88.

Chen S, Rotaru AE, Shrestha PM *et al*. Promoting interspecies electron transfer with biochar. *Sci Rep* 2014;**4**:1–7.

Cho CM, Mills JG. Kinetic formulation of the denitrification process in soil. *Can J Soil Sci* 1979;**59**:249–57.

Clough TJ, Condron LM, Kammann C *et al*. Review of biochar and soil nitrogen dynamics. *Agronomy* 2013;**3**:275–93.

Cornelissen G, Rutherford DW, Arp HPH *et al*. Sorption of pure N_2O to biochars and other organic and inorganic materials under anhydrous conditions. *Environ Sci Technol* 2013;**47**:7704–12.

Felgate H, Giannopoulos G, Sullivan MJ *et al*. The impact of copper, nitrate and carbon status on the emission of nitrous oxide by two species of bacteria with biochemically distinct denitrification pathways. *Environ Microbiol* 2012;**14**:1788–800.

Fungo B, Chen Z, Butterbach-Bahl K *et al*. Nitrogen turnover and N_2O/N_2 ratio of three contrasting tropical soils amended with biochar. *Geoderma* 2019;**348**:12–20.

Gaimster H, Alston M, Richardson DJ *et al*. Transcriptional and environmental control of bacterial denitrification and N_2O emissions. *FEMS Microbiol Lett* 2018;**365**:5.

Hagemann N, Joseph S, Schmidt HP *et al*. Organic coating on biochar explains its nutrient retention and stimulation of soil fertility. *Nat Commun* 2017;**8**:1089.

Hahnke1 SM, Moosmann P, Erb TJ *et al*. An improved medium for the anaerobic growth of *Paracoccus denitrificans* Pd1222. *Front Microbiol* 2014;**5**:18.

Harter J, Bustamante IG, Kuehfuss S *et al*. Gas entrapment and microbial N_2O reduction reduce N_2O emissions from a biochar-amended sandy clay loam soil. *Sci Rep* 2016;**6**:39574.

Harter J, El-Hadidi M, Huson DH *et al*. Soil biochar amendment affects the diversity of *nosZ* transcripts: Implications for N_2O formation. *Sci Rep* 2017;**7**:3338.

Harvey OR, Herbert BE, Kuo LJ *et al*. Generalized two dimensional perturbation correlation infrared spectroscopy reveals mechanisms for the development of surface charge and recalcitrance in plant derived biochars. *Environ Sci Technol* 2012;**46**:10641–50.

IPCC. *Climate Change 2014: Synthesis Report. Contribution of Working Groups I, II and III to the Fifth Assessment Report of the Intergovernmental Panel on Climate Change*. Core Writing Team, Pachauri RK, Meyer LA (eds). Geneva, Switzerland: IPCC, 2014.

Jiang J, Kappler A. Kinetics of microbial and chemical reduction of humic substances: implications for electron shuttling. *Environ Sci Technol* 2008;**42**:3563–9.

Kammann C, Ippolito J, Hagemann N *et al.* Biochar as a tool to reduce the agricultural greenhouse gas burden knowns, unknowns and future research needs. *J Environ Eng Landsc* 2017;**25**:114–39.

Kappler A, Wuestner ML, Ruecker A *et al.* Biochar as an electron shuttle between bacteria and Fe(III) minerals. *Environ Sci Technol Letter* 2014;**1**:339–44.

Kaur G, Kumar V, Arora A *et al.* Affected energy metabolism under manganese stress governs cellular toxicity. *Sci Rep* 2017;**7**:11645.

Keith A, Singh B, Singh BP. Interactive priming of biochar and labile organic matter mineralization in a smectite-rich soil. *Environ Sci Technol* 2011;**45**:9611–8.

Klüpfel L, Keiluweit M, Kleber M *et al.* Redox properties of plant biomass-derived black carbon (biochar). *Environ Sci Technol* 2014;**48**:5601–11.

Krause HM, Hueppi R, Leifeld J *et al.* Biochar affects community composition of nitrous oxide reducers in a field experiment. *Soil Biol Biochem* 2018;**119**:143–51.

Kučera I, Dadak V, Dobry R. The distribution of redox equivalents in the anaerobic respiratory chain of *Paracoccus denitrificans*. *Eur J Biochem* 1983;**130**:359–64.

Lehmann J, Joseph S. *Biochar for Environmental Management: Science and Technology*. London: Earthscan, 2009, 227–49.

Lehmann J. Bio-energy in the black. *Front Ecol Environ* 2007;**5**:381–7.

Lima AH, Mendonça JP, Duarte M *et al.* Reduced graphene oxide prepared at low temperature thermal treatment as transparent conductors for organic electronic applications. *Org Electron* 2017;**49**:165–73.

Liu X, Mao P, Li L *et al.* Impact of biochar application on yield-scaled greenhouse gas intensity: a meta-analysis. *Sci Total Environ* 2019;**656**:969–76.

Olaya-Abril A, Hidalgo-Carrillo J, Luque-Almagro VM *et al.* Exploring the denitrification proteome of *Paracoccus denitrificans* PD1222. *Front Microbiol* 2018;**9**:1137.

Prévoteau A, Ronsse F, Cid I *et al.* The electron donating capacity of biochar is dramatically underestimated. *Sci Rep* 2016;**6**:32870.

Quin P, Joseph S, Husson O *et al.* Lowering N_2O emissions from soils using eucalypt biochar: the importance of redox reactions. *Sci Rep* 2015;**5**:16773.

Ronsse F, Hecke S, Dickinson D *et al.* Production and characterization of slow pyrolysis biochar: influence of feedstock type and pyrolysis conditions. *GCB Bioenergy* 2013;**5**:104–15.

Sadasivam BY, Reddy KR. Adsorption and transport of methane in biochars derived from waste wood. *J Waste Manag* 2015;**43**:218–29.

Stouthamer AH. Bioenergetic studies on *Paracoccus denitrificans*. *Trends Biogeochem Sci* 1980;**5**:164–6.

Suliman W, Harsh J, Abu Lail N *et al.* Influence of feedstock source and pyrolysis temperature on biochar bulk and surface properties. *Biomass Bioenergy* 2016;**84**:37–48.

Sun T, Levin BDA, Guzman JJL *et al.* Rapid electron transfer by the carbon matrix in natural pyrogenic carbon. *Nat Commun* 2017;**8**:14873.

Sun X, Han X, Ping F *et al.* Effect of rice straw biochar on nitrous oxide emissions from paddy soils under elevated CO_2 and temperature. *Sci Total Environ* 2018;**628**:629–1009.

Sánchez-García M, Cayuela ML, Rasse DP *et al.* Biochars from mediterranean agroindustry residues: physicochemical properties relevant for C sequestration and soil water retention. *ACS Sustainable Chem Eng* 2019;**7**:4724–33.

Sánchez-García M, Sánchez-Monedero MA, Roig A *et al.* Compost vs biochar amendment: a two-year field study evaluating soil C build-up and N dynamics in an organically managed olive crop. *Plant and Soil* 2016;**408**:1.

Torres MJ, Simon J, Rowley G *et al.* Nitrous oxide metabolism in nitrate-reducing bacteria: physiology and regulatory mechanisms. *Adv Microb Physiol* 2016;**68**:353–432. Advances in Bacterial Electron Transport Systems and their Regulation. Poole (ed.), RK; Chapter 7.

Van Cleempt O, Patrick WH, Jr, McIlhenny RC. Formation of chemical and biological denitrification products in flooded soil at controlled pH and redox potential. *Soil Biol Biochem* 1975;**7**:329–32.

Weldon S, Rasse DP, Budai A *et al.* Biochar and denitrification: examining the effect of a biochar temperature series on the kinetics of gaseous N turnover. Which properties matter? *Soil Biol Biochem* 2019;**135**:173–83.

Wiedner K, Fischer D, Walther S *et al.* Acceleration of biochar of biochar surface oxidation during composting? *J Agric Food Chem* 2015;**63**:3830–7.

Wilhelm E, Batting R, Wilcock RJ. Low-pressure solubility of gases in liquid water. *Chem Rev* 1977;**77**:2.

Wu S, Fang G, Wang Y *et al.* Redox-active oxygen-containing functional groups in activated carbon facilitate microbial reduction of ferrihydrite. *Environ Sci Techol* 2017;**51**:9709–17.

Xu S, Adhikari D, Huang R *et al.* Biochar-facilitated microbial reduction of hematite. *Environ Sci Technol* 2016;**50**:2389–95.

Yang Z, Sun T, Subdiaga E *et al.* Aggregation-dependent electron transfer via redox-active biochar particles stimulate microbial ferrihydrite reduction. *Sci Tot Environ* 2020;**703**:135515.

Yuan H, Zhang Z, Lia M *et al.* Biochar's role as an electron shuttle for mediating soil N_2O emissions (Short communication). *Soil Biol Biochem* 2019;**133**:94–6.

Yuan Y, Bolan N, Prévoteau A *et al.* Applications of biochar in redox-mediated reactions. *Bioresour Technol* 2017;**246**:271–81.

Yu L, Wang Y, Yuan Y *et al.* Biochar as electron acceptor for microbial extracellular respiration. *Geomicrobiol J* 2016;**33**:530–6.

Zhang A, Cui L, Pan G *et al.* Effect of biochar amendment on yield and methane and nitrous oxide emissions from a rice paddy from Tai Lake plain, China. *Agr Ecosyst Environ* 2010;**139**:469–75.

Zhang P, Zheng S, Liu J *et al.* Surface properties of activated sludge-derived biochar determine the facilitating effects on *Geobacter* co-cultures. *Water Res* 2018;**142**:441–51.

Zhao L, Cao X, Mašek O *et al.* Heterogeneity of biochar properties as a function of feedstock sources and production temperatures. *J Hazard Mater* 2013;**256–257**:1–9